

Fabrication of GaN HEMTs with thin channel layer grown on AlN/SiC templates

Masatomo Sumiya^{1,*}, Osamu Goto², Yuki Takahara^{1,3}, Liwen Sang⁴, Yasutaka Imanaka⁵, Akira Uedono³, Taichiro Konno², Fumimasa Horikiri², Takeshi Kimura², and Hajime Fujikura²

¹ *Next Generation Semiconductor Group, National Institute for Materials Science, Tsukuba, Ibaraki 305-0044, Japan*

² *SCIOCS Co., Ltd., Hitachi, Ibaraki 319-1418, Japan*

³ *Division of Applied Physics, Faculty of Pure and Applied Sciences, University of Tsukuba, Tsukuba, Ibaraki 305-8571, Japan*

⁴ *International Center for Materials Nanoarchitectonics (MANA), National Institute for Materials Science (NIMS), Tsukuba, Ibaraki 305-0044, Japan*

⁵ *High Magnetic Field Measurement Group, National Institute for Materials Science, Tsukuba, Ibaraki 305-0003, Japan*

*Corresponding author. Email: SUMIYA.Masatomo@nims.go.jp

Abstract

We have grown GaN films on AlN/SiC templates for the fabrication of high electron mobility transistors (HEMTs) with thin GaN channel. GaN films with a step-terrace structure and smooth surface were obtained with a thickness of ~200 nm. The AlGaN/GaN (~400 nm) heterostructures were fabricated in a total growth time of 20 min without deposition of a thick and doped buffer layer. The interface quality was good enough for two-dimensional electron gas (2DEG) to exhibit Shubnikov-de Haas oscillation in the magnetic field at 1.8 K. The best mobility and sheet carrier density at room temperature were 2,100 cm²/Vs and 8.7×10¹² cm⁻², respectively. From C–V measurements, the carrier was pinch-off and no carriers were generated at the interface between the GaN and AlN layers. The GaN HEMTs with thin

channels on the AlN/SiC templates exhibited comparable properties to those on thick and highly resistive GaN buffer layers on SiC substrates. In view of both the shorter epitaxial-growth time and higher thermal conduction, the AlN/SiC templates were suitable for the fabrication of GaN HEMTs.

Group III-nitride semiconductor based electron devices are promising for high-power and high-frequency applications due to their superior electrical properties such as high electric field breakdown and high saturation electron velocity. AlGaN/GaN high electron mobility transistors (HEMTs) can also be used in high-frequency power amplifiers for long-distance and high-output power communication applications.¹

Conventional GaN HEMTs are prepared on Si or SiC substrates. To reduce the large mismatch in both the lattice constant and thermal expansion coefficient, $\text{Al}_x\text{Ga}_{1-x}\text{N}/\text{GaN}$ multilayers are deposited before depositing the GaN channel on Si substrate.² Epitaxial film growth is continuously carried out to obtain a thick GaN buffer layer with higher resistivity and lower dislocation density. A semi-insulating GaN buffer is necessary for GaN HEMTs because it reduces parallel conduction and ensures good channel pinch-off. To suppress the leakage in the GaN buffer layer, the residual carriers are often compensated by doping impurities of carbon^{3,4} or iron.^{5,6} The thickness of the GaN HEMT on SiC substrate is limited by the growth time to eliminate the influence of doping memory in a reactor.⁷ Since the heat dispersion is suppressed due to the thicker GaN buffer, the advantage of the higher thermal conductivity of SiC is diminished. Also, electrons trapped at the deep level defects caused by Fe, C, and intrinsic impurities can be injected into the AlGaN surface at a high operating voltage, which is the widely accepted model for explaining the current collapse.⁸ Regarding the cost of film growth, the thermal resistance, and the current collapse issue, it is important to obtain thin, high-quality GaN channel layers on SiC substrates without any compensation techniques.

We previously fabricated GaN films by direct growth on an AlN template/sapphire

substrate by using metalorganic chemical vapor deposition (MOCVD).⁹ Compared to GaN film grown on *c*-sapphire substrate, GaN film grown directly on an AlN template forms a smoother surface and better crystalline quality with a thinner thickness. Also, the AlGaN/InGaN/GaN heterostructure on the AlN template was good enough to exhibit Shubnikov-de Haas (SdH) oscillations from the two-dimensional electron gas (2DEG) of the InGaN channel at the interface of AlGaN/InGaN.¹⁰ The AlN layer has high resistivity and excellent thermal conductivity. If a thin GaN channel for electron transport can be directly grown on the AlN template/SiC substrate, it could potentially achieve short growth time, high heat dispersion, and lower impurities (suppression of current collapse) in the HEMT on SiC substrate.

In the present study, we developed a method for growing GaN films on an AlN template/SiC substrate, and investigated the behavior of the film growth to obtain a thin GaN channel layer suitable for HEMTs. The properties of the AlGaN/GaN heterostructure on the AlN template were evaluated with respect to the transport of electron in 2DEG in a magnetic field. GaN HEMTs were fabricated on the AlN templates and exhibited device properties comparable to those of conventional HEMTs despite the thin GaN channel.

We used AlN templates with a thickness of 0.3 μm grown by hydride vapor phase epitaxy on 6H-SiC substrate (SCIOCS Co., Ltd.). The lattice constants of *a*- and *c*- were 0.3118 and 0.4974 nm, respectively. The tensile strain was applied to the AlN/SiC template, and compared to that on *c*-sapphire (*a*: 0.3099 nm, *c*: 0,4990 nm). The full width at half maximum (FWHM) of the $\omega(0002)$ and $\omega(10\bar{1}2)$ rocking curve evaluated by X-ray

diffraction (XRD) was 160 and 310 arcsec, respectively. The surface of the AlN template had a rough appearance, as shown in Fig. 1(a), and the root mean square (RMS) estimated by atomic force microscopy (AFM) was 3.7 nm. GaN films were grown on the AlN template/SiC by metalorganic chemical vapor deposition (MOCVD) under atmospheric pressure after depositing the AlN layer on the template at the same temperature as that for GaN growth. GaN film was grown for various durations from 1 to 30 min at a growth rate of 2.4 $\mu\text{m}/\text{h}$ to investigate the growth behavior on the AlN template. The FWHM of the rocking curve of $\omega(0002)$ and $\omega(10\bar{1}2)$ was evaluated by XRD.

AlGaIn layers with various Al content and thickness were fabricated under 200 Torr after growing the GaN film with $\sim 0.4 \mu\text{m}$ of thickness to form AlGaIn/GaN heterostructure. The surface was capped with a GaN layer of several nanometers in thickness. The sheet carrier density and mobility were evaluated by Hall measurement (Hall System HL5500, Bio-Rad Laboratories Inc.). The C–V property of the device was measured using a Keysight B1500A semiconductor analyzer. The sample area was isolated with $6 \times 6 \text{ mm}^2$ by scribing the sample surface, and the van der Pauw method was used. Magneto-transport experiments in magnetic fields were performed for the AlGaIn/GaN heterostructures at the temperature of reduced-pressure helium to study the transport of 2DEG at the hetero interface. The ohmic contacts in the HEMT devices were formed by depositing conventional Ti/Al/Ni/Au metal stacks followed by rapid thermal annealing at 800 $^\circ\text{C}$ in an N_2 atmosphere. Gate metal deposition was done with a Ni/Au Schottky gate ($L_g = 20 \mu\text{m}$). The DC characteristics of the device were measured using an Agilent 4284A LCR analyzer and a Keithley 2636A SourceMeter.

Considering the rough surface morphology of the AlN template (Fig. 1(a)), similar to that of AlN/sapphire,⁹ we attempted to grow GaN film directly on the AlN/SiC templates. However, we did not obtain GaN film with a smooth surface. Although it was realized by the low-temperature buffer layer on the AlN/SiC template, the value of $\omega(0002)$ was larger than 300 arcsec. When an AlN layer was deposited on the AlN/SiC template at the same temperature as for GaN growth (990 °C), the AlN islands coalesced, exhibiting a smoother surface than that of the AlN template, as shown in Fig. 1(b). The thickness of the layer was approximately 80 nm. GaN film on the AlN layer grew laterally in the initial stage in Figs. 1(c) and (d), and exhibited a smooth surface at 6 min, as shown in Fig. 1(e). The thickness was approximately 220 nm, which was thinner for achieving a smooth surface similar to the GaN grown on the AlN/c-sapphire template.⁹ GaN films grown after depositing the AlN layer on the SiC substrate were flattened to a thinner thickness, as also reported in the literature.¹¹ After 30 min of growth ($\sim 1.2 \mu\text{m}$), a step-terrace structure was observed, and the RMS was 0.31 nm. The lattice constants a - and c - were 0.3190 and 0.5184 nm, respectively. A slight tensile strain was applied to the GaN, compared to GaN strained compressively on the AlN template/c-sapphire (a : 0.3182 nm, c : 0.5189 nm). The number of pits on the surface was $\sim 5.0 \times 10^8 \text{ cm}^{-2}$, corresponding to the dislocation density of the AlN template.

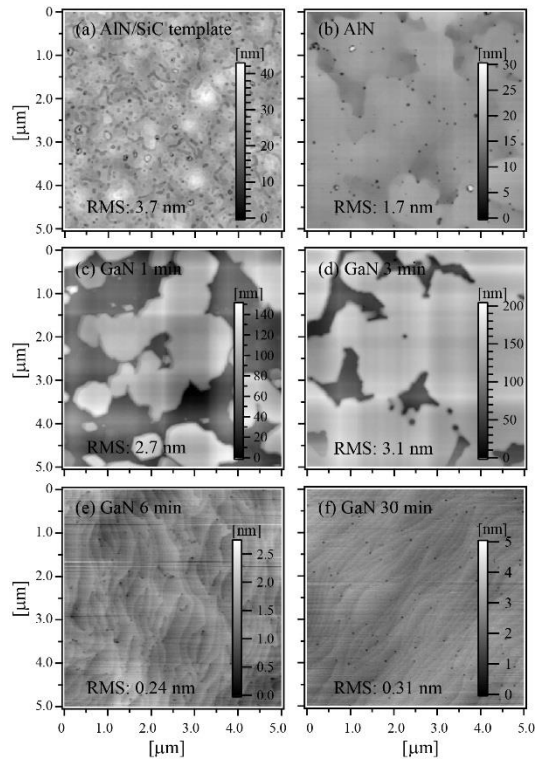


Fig. 1 AFM images of (a) AlN/SiC template, (b) AlN layer (80 nm) on the AlN template, and GaN films grown on AlN template for (c) 1 min, (d) 3 min, (e) 6 min, and (f) 30 min.

Figure 2 shows the variation in the FWHM for GaN on the AlN/SiC templates. The FWHM values decreased with an increase in the GaN growth time. The value of $\omega(10\bar{1}2)$ was lower than 300 arcsec for GaN grown for 600 s ($\sim 0.4 \mu\text{m}$). We deposited $\text{Al}_x\text{Ga}_{1-x}\text{N}$ barrier layers on the GaN layers with a thickness of $0.4 \mu\text{m}$ to fabricate the heterostructures as listed in Table 1.

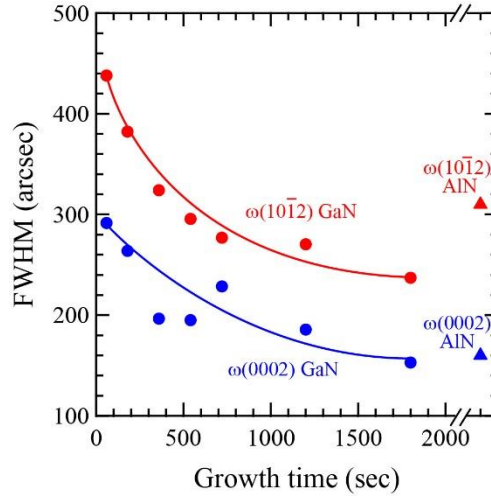


Fig. 2 Variation in the FWHM values of the $\omega(0002)$ and $\omega(10\bar{1}2)$ rocking curve as a function of the GaN growth time on the AlN/SiC templates.

Table 1 List of GaN HEMT heterostructures on AlN/SiC templates and the sheet resistance, mobility, and sheet carrier density. The AlN interlayer at the interface of AlGaIn/GaN was deposited for 5 s.

No.	GaN (nm)	GaN $\omega(10\bar{1}2)$ (arcsec)	AlGaIn Al comp./ thickness (nm)	GaN cap (nm)	Sheet resistance ($\Omega/\text{sq.}$)	Mobility (cm^2/Vs)	Sheet carrier density (cm^{-3})
A	400	330	0.22/24	2.0	336	1920	$8.7\text{e}12$
B	340	280	0.22/16	2.0	400	1690	$7.8\text{e}12$
C	-	289	0.23/16	-	371	1790	$8.5\text{e}12$
D	440	251	0.25/29	4.6	285	2100	$8.7\text{e}12$
E	330	301	0.22/15	5.0	367	1890	$7.4\text{e}12$
F	140	276	0.20/18	-	517	1780	$6.8\text{e}12$
G	400	330	0.23/19	1.2	-	5830*	$7.2\text{e}12^*$
H	400	309	0.20/17	1.2	-	5820*	$7.1\text{e}12^*$
I	400	350	0.20/20	1.4	-	6550*	$4.0\text{e}12^*$

* Evaluation from the SdH oscillation measured in the magnetic field at 1.8 K in Fig. 5.

Improving the FWHM values of $\omega(10\bar{1}2)$ was likely to enhance the mobility, as seen in the samples from *A* to *E*. Sample *D* exhibited the best mobility of 2,100 cm²/Vs and sheet carrier density of 8.7×10^{12} cm⁻². In Sample *F*, the mobility was 1,780 cm²/Vs despite the GaN channel layer of 140 nm. The sheet carrier density was also reduced to 6.8×10^{12} cm⁻² probably due to the decrease in thickness. The mobility and sheet carrier density were comparable to those of thicker GaN film on SiC substrate or GaN bulk described in previous reports.^{12,13,14}

Figure 3 shows the depth profile of the carrier density evaluated by C–V measurement for samples *G*, *H*, and *I*. Electrons were accumulated and 2DEG was formed at the heterointerface. In sample *H*, the carrier density increased at the depth of 150–200 nm. Although this abnormal carrier profile was sometimes observed (unknown origin), the carrier density decreased monotonically similar to samples *G* and *I*. It is worth noting that the carrier density was pinch off and that no carriers were generated at the interface between the GaN and AlN layers. It is considered that the energy levels of the defects at the interface were too deep to generate carriers. From secondary ion mass spectroscopy (SIMS), Si impurity was lower than 1.0×10^{16} cm⁻³ for both samples, and O impurity was 1.3×10^{17} and 2.5×10^{17} cm⁻³ for samples *G* and *I*, respectively. The oxygen impurity was attributed to the oxygen incorporated in the AlN template.¹⁵ The carbon impurity in sample *I* was $2\text{--}3 \times 10^{17}$ cm⁻³, which was one order of magnitude higher than that of sample *G*, because sample *I* was grown at a temperature 960 °C lower than that for sample *G*. Since the electrons in sample *I* were

compensated by carbon, the sheet carrier density was lower. On the other hand, the carbon concentration ($2\text{--}3\times 10^{16}\text{ cm}^{-3}$) in sample *G* was not enough to compensate the electrons from oxygen impurity. We suppose that part of the hydrogen in sample *G* ($7\times 10^{17}\text{ cm}^{-3}$) positively charged could be trapped at Ga vacancies and play an acceptor-like role to compensate the electrons, as predicted by Van de Walle.¹⁶

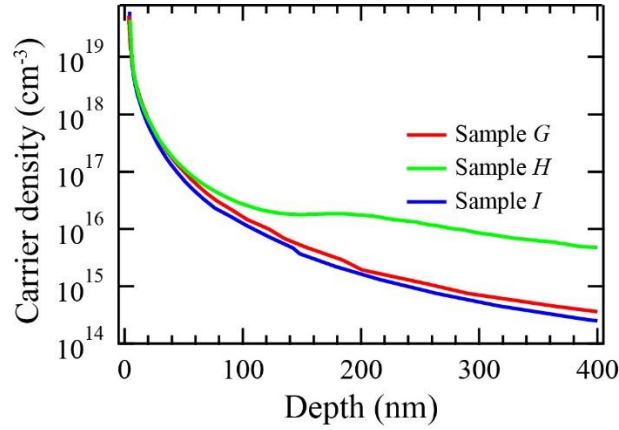


Fig. 3 Carrier depth profiles evaluated by C–V measurement for samples *G* (red), *H* (green), and *I* (blue).

To understand the interface quality, the carrier transport was investigated under a magnetic field at low temperature for the three samples. The carriers generated from the impurities or defects in GaN or AlGa_N were frozen out at low temperature, which suppressed the parallel conduction in the GaN and/or AlGa_N layer. Although the GaN channel layer was as thin as 0.4 μm, the heterointerface at the AlGa_N/GaN for all samples was so fine that the SdH oscillation of 2DEG transport was observed in the magnetic field up to 15 T at 1.8 K, as shown in Fig. 4(a). The mobility of the 2DEG can be roughly estimated from the crossover magnetic field between the magneto resistance (R_{xx}) and the Hall resistance (R_{xy}). Sample *I*

exhibits the highest mobility (lowest sheet carrier density).

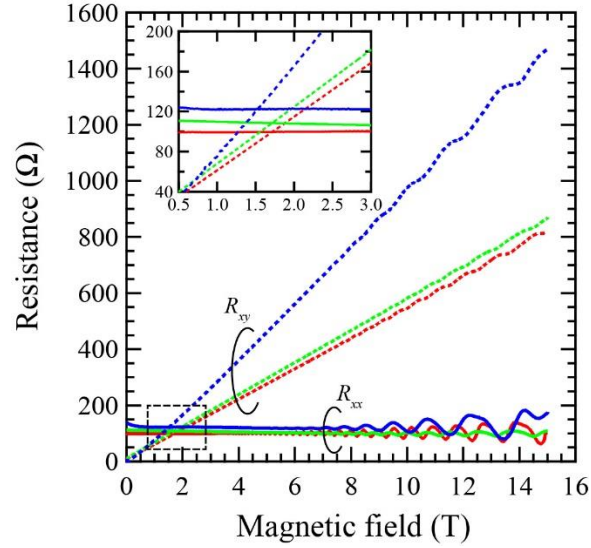


Fig. 4 Magneto-transport measurements for samples *G* (red), *H* (green), and *I* (blue) at high magnetic fields up to $B = 15$ T at 1.8 K. Inset shows the expanded plot near the cross point and R_{xx} and R_{xy} .

Schottky-type HEMT devices were fabricated on samples *G*, *H*, and *I* with a gate width (W_G) of 200 μm and a gate length (L_G) of 20 μm without a field plate and surface passivation. Figure 5(a) and 5(b) shows the drain I - V characteristics and the transconductance (g_m) at $V_{DS} = +15$ V of the GaN HEMT of sample *H*, respectively. Although the self-heating effect was observed in the saturation region, the HEMT device exhibited the conventional I - V characteristics. The maximum current density was 480 mA/mm and the on-resistance was 15.1 Ω mm. The peak value of g_m at $V_{DS} = +15$ V was 81 mS/mm. The current on/off ratio was $\sim 10^5$. Table 2 outlines the device structures and properties together with those from the literature, although the number of reports for GaN HEMT on SiC is not high. Although

sample *H* exhibited abnormal C–V properties, the HEMT properties were conventional. Sample *I* showed a higher on-resistance (R_{on}) of the device, reflecting a lower mobility and sheet carrier density. Despite the absence of a thick, highly resistive GaN buffer layer, the GaN HEMTs with a thin GaN channel exhibited comparable properties to those of thick GaN buffer layers on SiC with respect to the value of g_m . The properties are expected to be improved by modifying the device processes such as passivation and contact.

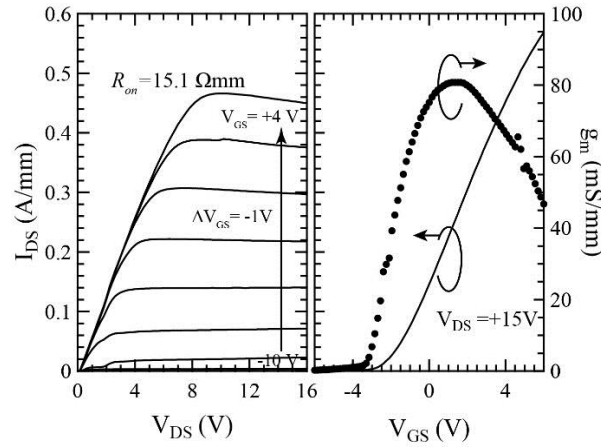


Fig. 5 (a) Drain I–V characteristics, (b) transfer characteristics under $V_{DS} = 15$ V for the GaN HEMT device fabricated from sample *H*.

Table 2 Comparison of the GaN HEMTs in this study with the device structures and properties on SiC substrates from the references.

No. (Ref.)	GaN buffer (μ m)	GaN channel (nm)	AlGaIn Al comp/ thickness (nm)	g_m (mS/mm)	V_{th} (V)	R_{on} (Ω mm)
Sample <i>G</i>	no	400	0.23/19	80	-1.8	14.3
Sample <i>H</i>	no	400	0.20/17	81	-2.0	15.1
Sample <i>I</i>	no	400	0.20/20	77	-1.5	19.7
Ref.17	GaN (2.0)	-	0.22/22	120	-4.0	7.0

Ref.18	GaN:Fe (3.0)	500	0.24/18	95	-4.0	16.0
Ref.19	GaN:C (-)	1800	0.25/25	280*	-2.0	2.6
Ref.20	GaN:Fe (0.3)	900	-/18	-	-1.5	5.8

* Gate length: 0.2 μm .

In summary, GaN films were grown on AlN/SiC templates for the fabrication of GaN HEMTs with a thin GaN channel. After depositing the AlN layer, the lateral growth of GaN nuclei was enhanced, and the formation of the surface with a step-terrace structure took place for a thickness of ~ 200 nm. The FWHM value of $\omega(10\bar{1}2)$ was lower than 300 arcsec for GaN grown for 600 s (~ 400 nm). The AlGaN/GaN heterostructures were fabricated in 20 min, and were good enough for the 2DEG to exhibit SdH oscillation in the magnetic field at 1.8 K. The mobility and sheet carrier density at room temperature were $2,100 \text{ cm}^2/\text{Vs}$ and $8.7 \times 10^{12} \text{ cm}^{-2}$, respectively. From the C–V measurement, the carrier density was pinch-off and no carriers were generated at the interface between the GaN and AlN layers. The GaN HEMTs with a thin channel on the AlN/SiC templates exhibited comparable properties to those on thick, highly resistive GaN buffer layers on SiC substrates.

Acknowledgement

This study was partially supported by TIA Kakehashi.

Data availability statement

The data that support the findings of this study are available from the corresponding author upon reasonable request.

References

- ¹ M. Micovic, D. F. Brown, D. Regan, J. Wong, Y. Tang, F. Herrault, D. Santos, S. D. Burnham, J. Tai, E. Prophet, I. Khalaf, C. McGuire, H. Bracamontes, H. Fung, A. K. Kurdoghlian, A. Schmitz, '*High Frequency GaN HEMTs for RF MMIC Applications*', Technical Digest - International Electron Devices Meeting, IEDM 7838337, 3.3.1 (2017).
- ² M. Sumiya., Y. Kamo, N. Ohashi, M. Takeguchi, Y. U. Heo, H. Yoshikawa, S. Ueda, K. Kobayashi, T. Nihashi, M. Hagino, T. Nakano, S. Fuke, '*Fabrication and hard X-ray photoemission analysis of photocathodes with sharp solar-blind sensitivity using AlGaN films grown on Si substrates*', Appl. Surf. Sci. **256**, 4442 (2010).
- ³ M. J. Uren '*Buffer Design to Minimize Current Collapse in GaN/AlGaN HFETs*', IEEE Trans. Electron Devices **59**, 3327 (2012).
- ⁴ S. Besendörfer, E. Meissner, T. Zweipfennig, H. Yacoub, D. Fahle, H. Behmenburg, H. Kalisch, A. Vescan, J. Friedrich, and T. Erlbacher, '*Interplay between C-doping, threading dislocations, breakdown, and leakage in GaN on Si HEMT structures*' AIP Advances **10**, 045028 (2020).
- ⁵ M. Meneghini, I. Rossetto, D. Bisi, A. Stocco, A. Chini, Al. Pantellini, C. Lanzieri, A. Nanni, G. Meneghesso, and E. Zanoni, '*Buffer Traps in Fe-Doped AlGaN/GaN HEMTs: Investigation of the Physical Properties Based on Pulsed and Transient Measurements*', IEEE Trans. Electron Devices, **61**, 4070 (2014).
- ⁶ J. Chu, Q. Wang, C. Feng, L. Jiang, W. Li, H. Liu, Q. Wang, H. Xiao, and X. Wang, '*Abnormal increase of 2DEG density in AlGaN/GaN HEMT grown on free-standing GaN substrate*' Jpn. J. Appl. Phys. **60**, 035506 (2021).
- ⁷ D. Zhang, Z. Li, Q. Yang, D. Peng, C. Li, W. Luo, X. Dong, '*Research on epitaxial of 250 nm high quality GaN HEMT based on AlN surface leveling technology*' Appl. Surf. Sci.

509, 145339 (2020).

⁸ R. Vetury, N.Q. Zhang, S. Keller, U.K. Mishra, '*The impact of surface states on the DC and RF characteristics of AlGa_N/Ga_N HFETs*', IEEE Trans. Electron Devices **48**, 560 (2001).

⁹ M. Sumiya, K. Fukuda, S. Yasiro, T. Honda, '*Influence of thin MOCVD-grown Ga_N layer on underlying AlN template*' J. Crys. Growth **532**, 125376 (2020).

¹⁰ M. Sumiya, D. Kindole, K. Fukuda, S. Yashiro, K. Takehana, T. Honda, Y. Imanaka, '*Growth of AlGa_N/InGa_N/Ga_N Heterostructure on AlN Template/Sapphire*' Phys. Status Solidi B **257**, 1900524 (2020).

¹¹ D. Zhang, Z. Li, Q. Yang, D. Peng, C. Li, W. Kuo and X. Dang, '*Research on epitaxial of 250 nm high quality Ga_N HEMT based on AlN surface leveling technology*', Appl. Surf. Sci. **509**, 145339 (2020).

¹² J.-T. Chen, C.-W. Hsu, U. Forsberg, and E. Janzen, '*Metalorganic chemical vapor deposition growth of high-mobility AlGa_N/AlN/Ga_N heterostructures on Ga_N templates and native Ga_N substrates*', J. Appl. Phys. **117**, 085301 (2015).

¹³ K. Narang, R. K. Bag, V. K. Singh, A. Pandey, S. K. Saini, R. Khan, A. Arora, M. V. G. Padmavati, R. Tyagi, and R. Singh, '*Improvement in surface morphology and 2DEG properties of AlGa_N/Ga_N HEMT*', J. Alloys Comp. **815**, 152283 (2020).

¹⁴ J. Chu, Q. Wang, C. Feng, L. Jiang, W. Li, H. Liu, Q. Wang, H. Xiao, and X. Wang, '*Abnormal increase of 2DEG density in AlGa_N/Ga_N HEMT grown on free standing Ga_N substrate*', Jpn. J. Appl. Phys. **60**, 035506 (2021).

¹⁵ Z. Chen, Y. Pei, S. Newman, R. Chu, D. Grown, R.Chung, S. Keller, S. P. Denbaars, S. Nakamura, and U. K. Mishra, '*Growth of AlGa_N/Ga_N heterojunction field effect transistors*

-
- on semi-insulating GaN using AlGaN interlayer*’, Appl. Phys. Letts. **94**, 112108 (2009).
- ¹⁶ C. G. Van de Walle and J. Neugebauer, ‘*Universal alignment of hydrogen levels in semiconductors, insulators and solutions*’ Nature **423** 626 (2003).
- ¹⁷ J. Xu, R. Wang, L. Zhang, S. Zhang, P. Zheng, Y. Zhang, Y. Song, and X. Tong, ‘*Early stage degradation related to dislocation evolution in neutron irradiated AlGaN/GaN HEMT*’, Appl. Phys. Letts. **117**, 023501 (2020).
- ¹⁸ K. Lie, H. Y. Wang, H. C. Chiu, Y. Chen, D. Li, C. R. Huang, H. L. Kao, H. C. Kuo, S. W. H. Chen, ‘*Analysis of the back-barrier effect in AlGaN/GaN high electron mobility transistor on free-standing GaN substrates*’, J. Alloy and Comp. **814** 152293 (2020).
- ¹⁹ X. Li, J. Brgsten, D. Nilsson, O. Daniesson, H. Pedersen, N. Rorsman, E. Janzen, and U. Forsberg, ‘*Carbon doped GaN buffer layer using propane for high electron mobility transistor applications: Growth and device results*’, Appl. Phys. Letts. **107**, 262105 (2015).
- ²⁰ Q. Ma, T. Yoshida, Y. Ando, and A. Wakejima, ‘*Transient response of drain current following biasing stress in GaN HEMTs on SiC substrate with a field plate*’, Jpn. J. Appl. Phys. **59**, 101002 (2020).